Optik - International Journal for Light and Electron Optics 252 (2022) 168576

Contents lists available at ScienceDirect

Optik

journal homepage: www.elsevier.com/locate/ijleo

Optical and photonic properties dependence on HNMB solvents: An emitter molecule for OLEDs

Emine Tanış

Department of Electrical Electronics Engineering, Kırşehir Ahi Evran University, 40100 Kırsehir, Turkey

ARTICLE INFO

Keywords:
HNMB
Organic light emitting diodes
Optoelectronic
Photonic

ABSTRACT

The development of organic light-emitting diodes (OLEDs) is very important due to their use in new generation lighting and displays, their color resolution and their unique optical properties. Herein, the change of the electronic and optical properties of a new molecule, 4-[(*E*)-[(2-hydroxy-1-naphthalenyl)methylene]amino]-3-methyl benzoic acid (HNMB) in different solvents are reported by experimental and advanced theoretical calculations. Optical properties are investigated by calculating the optical absorption wavelength, optical refractive index, optical band gap, optical conductance, angle of incidence, angle of refraction, contrast for different solvents. Finally, due to well-suited photonic and optoelectronic properties, the HNMB can be used as a phosphorescent and OLED material.

1. Introduction

In recent years, materials containing organic molecules have gained great importance in terms of materials science [1–3]. These materials are considered to be good candidates for optoelectronic, photovoltaic and mechanochromic luminescent device research [4,5]. Because of their conjugated electrons, organic materials have improved efficiency, stability, and flexibility [6,7].

OLED is designed as a layer of organic material placed between two electrodes called anode and cathode, and in this organic layer with delocalized pi electrons, the pi-electron conductivity is between the insulator and the conductor, and so it is used as a semiconductor [8]. Similarly, organic semiconductor molecules are used in many fields of science and technology due to their unique optical and charge transfer properties. Therefore, the determination of optical properties is very important in terms of technological applications. OLEDs have a wide range of uses, such as smart watches and TV screens, sensors, lighting devices, and sensor applications [9].

HNMB is a commercial molecule important for mechanochromatic luminescent and OLED materials. Mechanochromic luminescent materials are very sensitive to pressure. Zhang et al. [10] synthesized the (E)-4-((2-hydroxynaphthalen-1-yl) methylene) amino)-3 methylbenzoic acid molecule (HNMB), and its charge transfer, emission properties, and reliability in pressure sensor applications were investigated.

The solvent is an essential complement to the active medium. Because it is known that solvent organic molecules significantly change their structural and optical properties [11–13]. Therefore, solvent environments that cause strong changes in the properties of materials significantly affect the performance of the designed devices [14].

In this study, the electronic (the UV-Vis absorption spectra, HOMO, LUMO, and HOMO-LUMO gap (Eg) energies), optical (optical band gap (Eg), refractive index, reflectivity, and optical conductivity) and photonic properties (angle of incidence (Φ_1), refraction

E-mail address: eminetanis@ahievran.edu.tr.

https://doi.org/10.1016/j.ijleo.2022.168576
Received 10 June 2021; Received in revised form 24 December 2021; Accepted 3 January 2022
Available online 5 January 2022

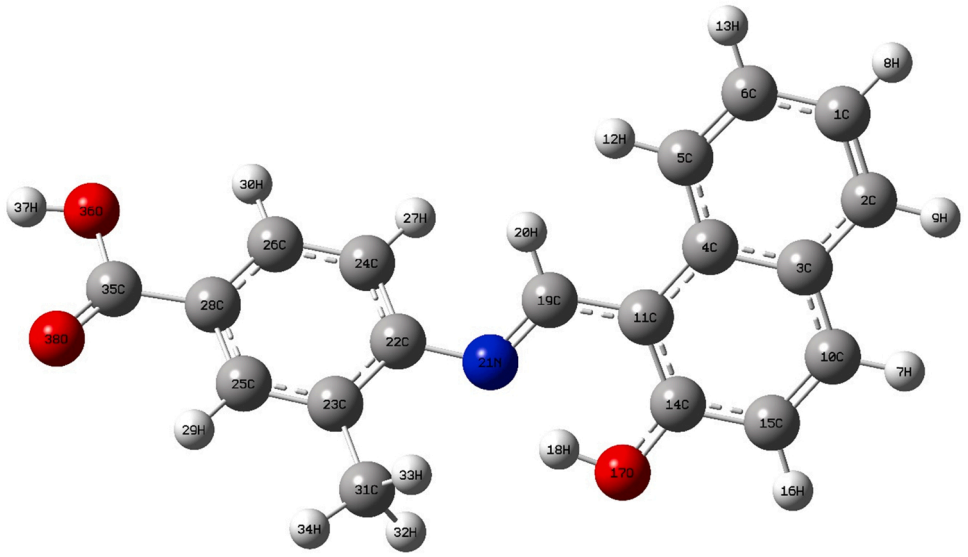

Fig. 1. The optimized structure of HNMB.

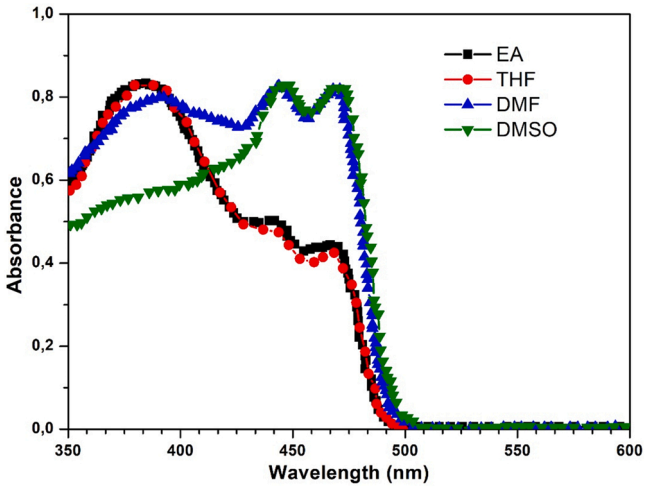

Fig. 2. Experimental absorbance spectra of HNMB for different solvents (The data are taken from the experimental study of Ref. [6]).

angle (Φ_2), and contrast (α_c) of the HNMB molecule in various solvents (ethyl acetate (EA), tetrahydrofuran (THF), dimethyl sulfoxide (DMSO) and dimethyl formamide (DMF)) were investigated by the TD-DFT method and experimental measurements. The available experimental results have been compared with theoretical values.

2. Computational details

The calculations of the HNMB have been performed using the Gaussian 09 [15] and Gauss View 5.0 [16] programs. Electronic and optical calculations of the optimized molecule using the TD-DFT/LSDA function with the aug-cc-pVDZ basis set were also performed on the same model method. The TD-DFT method is known to be one of the most reliable methods for calculating the electronic structure of molecules in solid-state [17–22]. The optimized structure used in quantum chemical calculations is given in Fig. 1. After optimization, electronic calculations were made for all solvents to compare with the experimental absorbance values.

3. Results and discussion

3.1. Electronic properties

The experimental absorbance data [10] of the HNMB molecule in EA, THF, DMSO, and DMF solvents is shown in Fig. 2. The

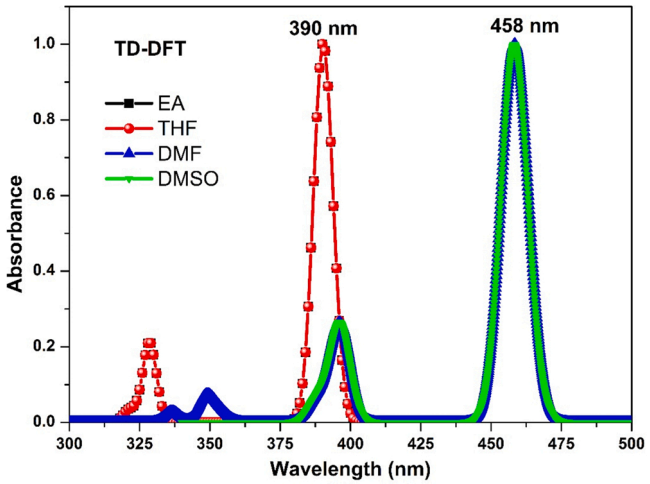

Fig. 3. Theoretical absorbance spectra of HNMB for different solvents.

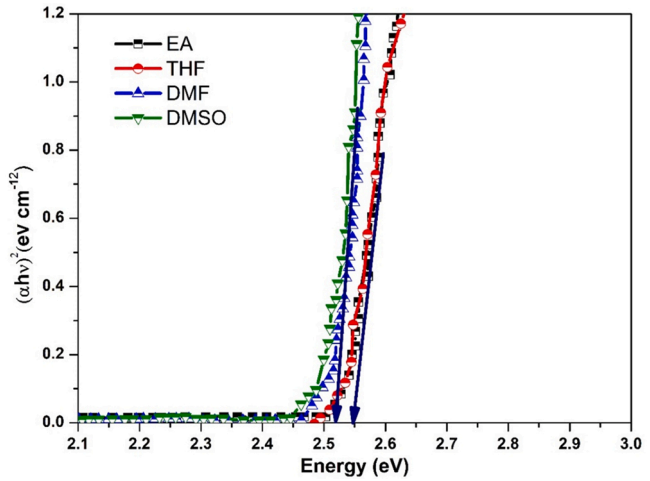

Fig. 4. The experimental $(\alpha h\vartheta)^2$ curves vs. photon energy (E) of the HNMB for different solvents.

absorbance spectrums of HNMB were observed at approximately 383 nm (3.24 eV) in EA and THF solvents, while maximum peaks were observed at 439 (2.82 eV) and 465 nm (2.66 eV) in DMF and DMSO, respectively. It is understood from these results that HNMB has maximum absorbance peaks in the visible region for all solvents. In addition, the HNMB molecule absorbs the violet in EA and THF solvents, while it absorbs the blue in DMF and DMSO solvents. A solvent with a large dielectric constant creates more stabilization energy for polar species [23]. The stabilizing effect of solvents decreases depending on the dielectric constant, such as DMSO ($\varepsilon = 46.7$), DMF ($\varepsilon = 36.7$), THF ($\varepsilon = 7.58$) and EA ($\varepsilon = 6.02$), respectively. The blue shift of the absorbance spectrum defining negative solvatochromism is because the polarity of DMSO and DMF solvents is greater than that of EA and THF solvents. PMMA and CdS nanocomposites modify the band gap so that it has high absorption in the range of 190–330 nm and transmits it into the visible range (360–1100 nm), suitable for OLED applications. Some optical and electrical parameters of PMMA and its metal sulfide-based polymeric nanocomposites are given in [24–26].

Theoretical UV calculations were done by using the TD-DFT/LSDA method and the aug-cc-pVDZ basis set. As can be seen from Fig. 3, the maximum absorbance is 390 nm (3.18 eV) for EA and THF and 458 nm (2.71 eV) for DMF and DMSO. These results are good enough to compare with experimental results. Small differences between the theoretical results and the experimental results may be because the solvents may not have been completely separated from the HNMB molecule under the experimental measurement conditions.

The energy difference between the frontier orbital levels of the highest occupied orbital (HOMO) and the lowest unoccupied orbital (LUMO) determines the band gap value. From the band gap, it is understood that HNMB is a 2.55 eV semiconductor material. This band gap is also clearly compatible with Rubrene [27] and 4,5-bis(benzofuro[3,2-*c*] carbazole-5-yl) phthalonitrile [28], both of which are OLED materials.

Table 1
The E_g values of the HNMB for different solvents.

Solvents	E_g (eV)
EA	2.55
THF	2.55
DMF	2.51
DMSO	2.51

Table 2
The experimental (Exp.) refractive index (n) parameters and Moss (M), Ravindra (Ra), Herve-vandamme (H-V), Reddy (Re) and Kumar-Singh (K-S) relations results of the HNMB for different solvents.

Solvents	Exp	Ra	H-V	M	Re	K-S
EA	1.93	2.50	2.47	2.50	2.89	2.49
THF	2.06	2.50	2.47	2.50	2.89	2.49
DMF	1.79	2.52	2.48	2.52	2.91	2.50
DMSO	1.72	2.52	2.48	2.52	2.91	2.50

3.2. Optical properties

The optical band gap is an important optical parameter that controls the nature of the electroluminescence signal in OLEDs. It can be calculated with the help of the Tauc relation [29];

$$(\alpha h\nu) = A\left(h\nu - E_g\right)^n \tag{1}$$

where α is the absorption coefficient, A is a constant, hν is photon energy, E_g is the optical energy gap, and n is a parameter that measures the types of the bandgap. For HNMB, the type of bandgap [30] is the direct allowed bandgap (E_g). For this, we plotted the $(\alpha h\nu)^2$ plot vs E of the HNMB for EA, THF, DMF and DMSO solvents, and as seen in Fig. 4. We calculated the E_g values from the linear regions of Fig. 4 and obtained E_g values of the HNMB for EA, THF, DMF and DMSO solvents were given in Table 1. As can be seen from Table 1, the E_g value of HNMB was approximately 2.55 eV for EA and THF, and approximately 2.51 eV for DMF and DMSO. These results are very close to the results of metal oxide nanocomposites such as PMMA/TiO2 [31–33], PMMA/CuO [34], which have an important place in optoelectronic device applications. Also, the theoretically obtained energy gap of 2.55 eV, which is the difference between HOMO and LUMO, is very compatible with the experimental optical band gap values of the HNMB.

The optical refractive index (n) is an important value for optoelectronics, as it shows how the frequencies and wavelengths of light change as they pass through the transparent material. The experimental n values can be determined by [35],

$$n = \left\{ \left[\frac{4R}{(R-1)^2} - k^2 \right]^{1/2} - \frac{R+1}{R-1} \right\} \tag{2}$$

and are given in Table 2. As can be seen from the table, the lowest experimental refractive index is 1.72 in DMSO solvent and the highest is 2.06 in THF solvent. When the experimentally determined refractive index values are compared with those of PMMA/TiO2, a metal oxide nanomaterial [31–33], it is understood that HNMB is quite suitable for applications such as OLED and solar cells. Depending on the band gap E_g, the quasi-experimental refractive index values are calculated with the help of the following equations proposed by Moss, Ravindra, Herve-Vandamme, Reddy and Kumar and Singh presented in Table 2.

Moss relation can be expressed as follow [36]:

$$n^4 E_g = 95 \quad eV \tag{3}$$

Ravindra proposed the following relationship [37]:

$$n = 4.084 - 0.62E_g \tag{4}$$

Herve-Vandamme relation [38].

$$n = 1 + \left(\frac{A}{E_g + B}\right)^2 \tag{5}$$

Here, A= 13.6 eV is a constant parameter like hydrogen ionization energy. B = 3.47 eV and represents the difference between the band gap and ultraviolet resonance energy.

Reddy relation [39]

$$n^4\left(E_g - 0.365\right) = 154 \tag{6}$$

The following relationship was used to calculate Kumar and Singh's relationship [40]:

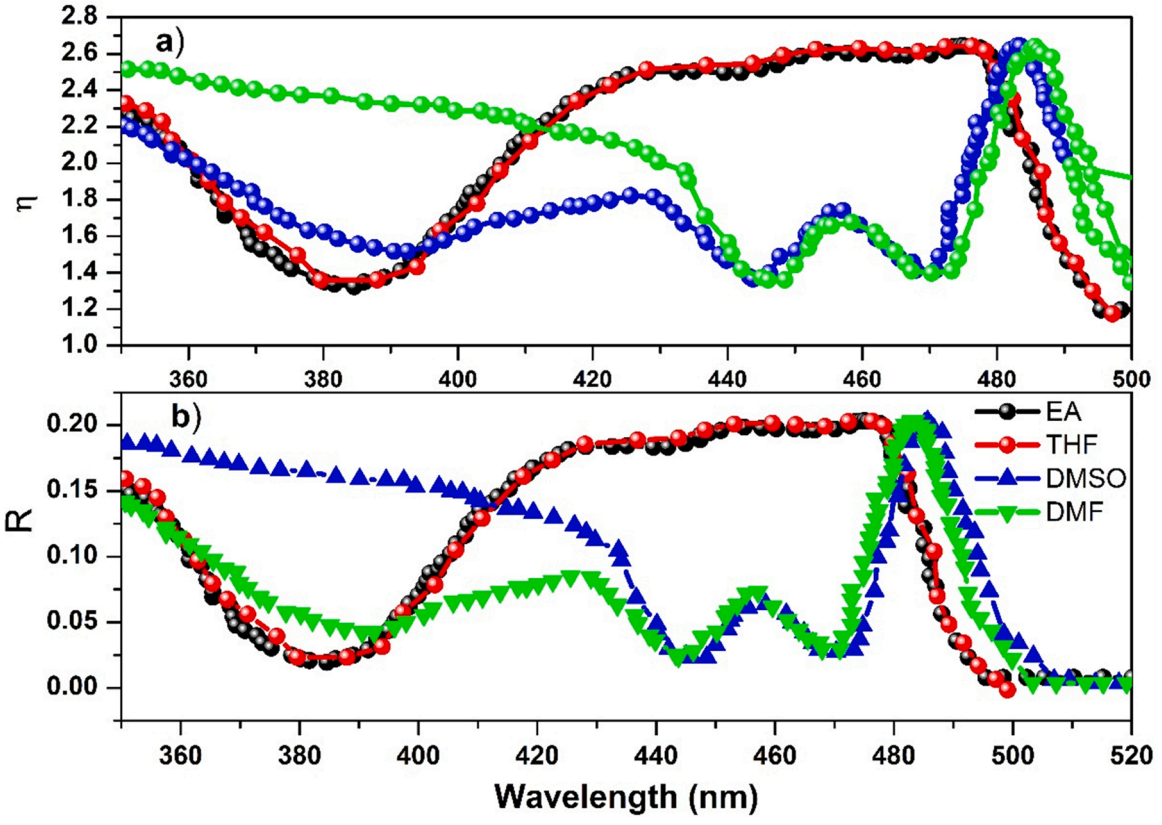

Fig. 5. (a) The experimental refractive index; (b) reflectivity of HNMB for different solvents.

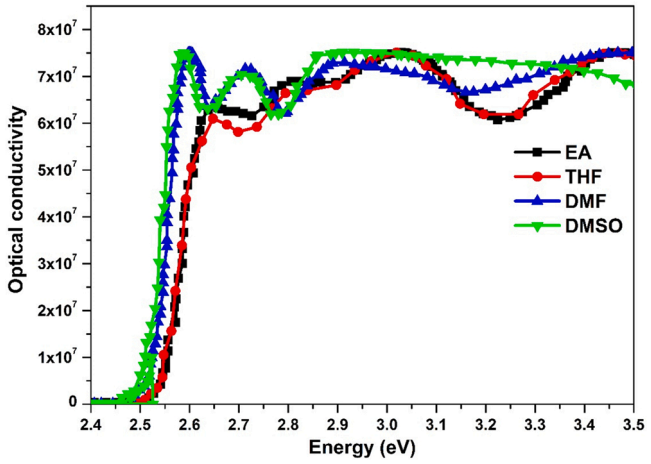

Fig. 6. The experimental optical conductivity of HNMB for different solvents.

$$n = KE_g^C \tag{7}$$

where K = 3.3668 and C = − 0.32234 are constant parameters.

It is seen that these values obtained by quasi-experimental relations are larger than the experimental refractive indices, and the Herve-Vandamme results are the closest to the experimental results. Fig. 5 shows the experimental refractive index (a) and experimental reflectivity (b) as a function of wavelength. Maximum peaks are observed in Fig. 5-(a) at 477 nm for EA and THF solvents, and at 485 nm for DMF and DMSO solvents. After the maximum peaks, the refractive index values of all solvents decreased rapidly.

The reflectivity peaks of HNMB in EA, THF, DMSO, and DMF solvents are shown in Fig. 5-(b) at 477, 477, 482, and 485 nm,

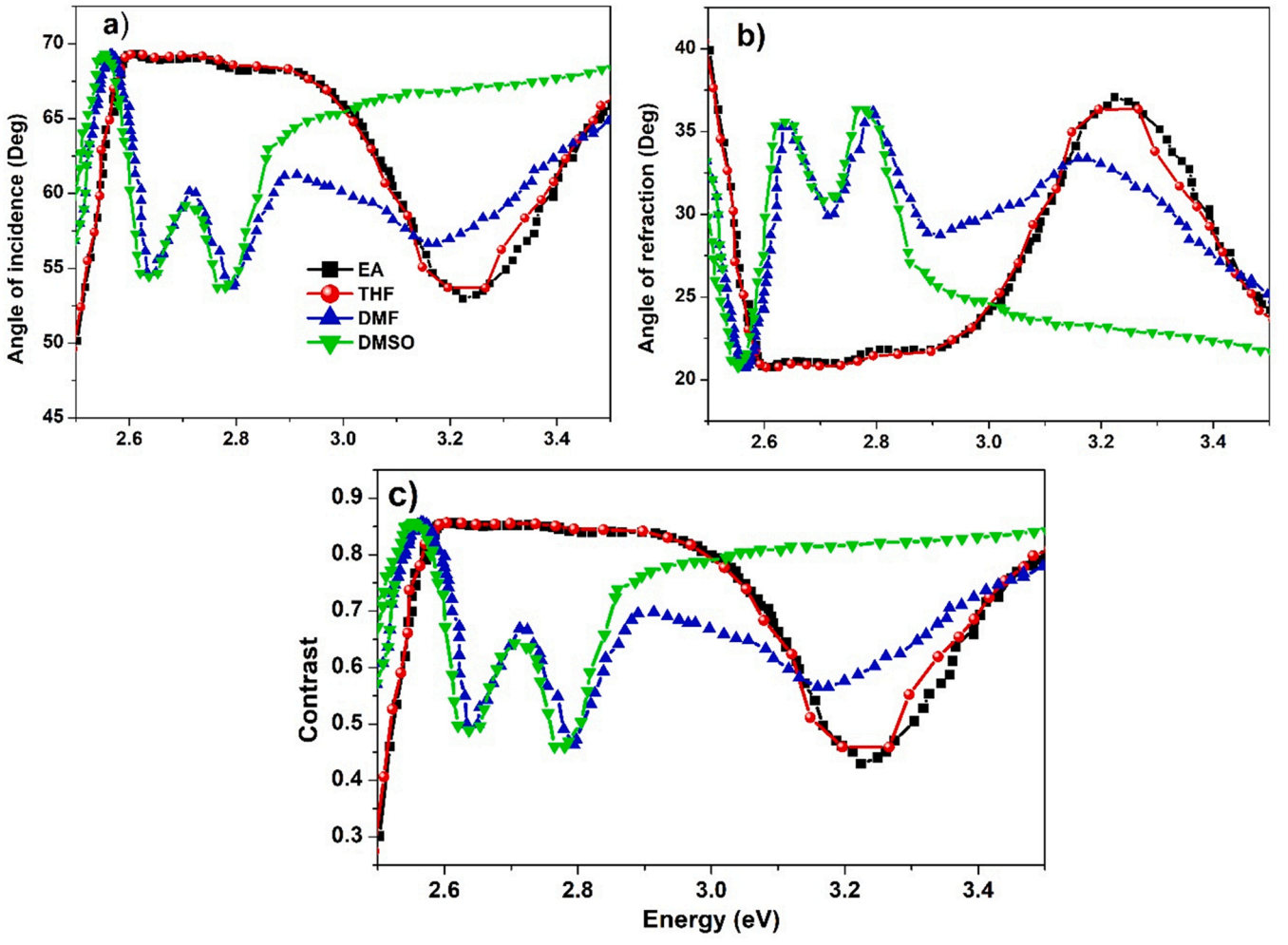

Fig. 7. The experimental (a) angle of incidence; (b) angle of refraction; (c) contrast of HNMB for different solvents.

respectively. It is seen that HNMB reflects about 20% of the incident light for all solvents at these wavelengths. Both the refractive index and the reflectivity decrease after these wavelengths. Furthermore, Fig. 5-(b) shows that the reflectivity of HNMB increases from 1% to 20% in the 384–477 nm range in EA and THF solvents, and from 2% to 10% in the 470–484 nm range in DMF and DMSO solvents. It is more suitable for OLED applications because the reflectivity is low in the visible region range, causing an increase in the contrast [41,42].

Fig. 6 shows the change of optical conductivity in related solvents depending on the photon energy. It can be seen from the figure that when the photon energy is equal to the band gap of HNMB, there is a sudden increase in optical conductivity. It is also understood that HNMB has higher optical conductivity in DMF and DMSO solvents than in EA and THF solvents. Therefore, it can be said that the decrease in the bandgap increases the optical conductivity. In addition, the optical conductivity results are compatible with the results of the phosphor bipolar base material as a light-emitting layer in the design of OLED devices [43].

3.3. The photonic properties

The properties of optoelectronic materials such as angle of incidence (Φ_1), refraction angle (Φ_2), and contrast (α_c) are very important [44]. Φ_1, Φ_2 can be given as the following formulas (8) and (9);

$$\Phi_1 = \tan^{-1}\left(\frac{n_2}{n_1}\right) \tag{8}$$

$$\Phi_2 = \sin^{-1}\left(\left(\frac{n_1}{n_2}\right)\sin\Phi_1\right) \tag{9}$$

where n_1 defines the refractive index of the medium, n_2 defines the refractive index of the PHMB. Fig. 7(a, b) shows the variation of incidence and refraction angle values in respective solvents as a function of energy. The Φ_1 values of HNMB for EA, THF, DMF, and DMSO can be seen in Fig. 7a, where the material has the highest peak in the optical band value in the respective solvent. The energy-dependent changes of Φ_2 values obtained by using Eq. (8) are shown in Fig. 7b. In contrast to the Φ_1 change in Fig. 7a, Φ_2 appears to have a minimum scattering angle at optical band gap values in all solvents. Also, HNMB's Φ_1 values are higher than Φ_2 values. In the previous study [43], incidence and refractive angle values in the visible region range were lower than the results here.

Contrast, which is an important value for determining the sensitivity of HNMB, is calculated by the following formula [45]. The versus of the contrast varies with energies and solvents is given in Fig. 7c. As shown in this figure, While the lowest contrast value was obtained at approximately 3.22 eV in EA and THF solvents, the highest value was obtained in DMF and DMSO solvents at 2.55 eV. Our contrast values are very close to the contrast values of the 26DczPPy material known for its application to high-tech devices [46].

$$\alpha_c = 1 - \left(\frac{n_1}{n_2}\right)^2 \tag{10}$$

4. Conclusion

Changes in electronic, optical and photonic properties of HNMB for various solvents were studied in detail. HNMB is a direct bandgap semiconductor (2.51 eV in DMF and DMSO solvents, 2.55 eV in EA and THF solvents). The energy gap value (2.55 eV) between HOMO and LUMO is quite compatible with this measured direct band gap. HNMB absorbs violet and blue due to solvents. The negative solvatochromism data were observed concerning the solvent polarity. HNMB is a sample with low reflectivity in all solvents. From the experimental and theoretical results, It can be understood that HNMB can be used in photonic and optoelectronic technology with its excellent optical and photonic properties.

Declaration of Competing Interest

The author declares no conflicts of interest.

Acknowledgements

The numerical calculations reported in this paper were performed at the TUBITAK ULAKBIM, High Performance and Grid Computing Center (TRUBA resources). The author would like to thank TUBITAK ULAKBİM and High Performance and Network Computing Center for the numerical calculations used in this article. Also thanks to Prof. Mengyao Zhang and colleagues from the Chemistry Department of Capital Normal University for the absorbance data.

Ethical Procedure

- The research meets all applicable standards with regard to the ethics of experimentation and research integrity, and the following is being certified/declared true.

- As an expert scientist and along with co-authors of concerned field, the paper has been submitted with full responsibility, following due ethical procedure, and there is no duplicate publication, fraud, plagiarism, or concerns about animal or human experimentation.

A Disclosure/Conflict of Interest Statement

- The author of this paper has a financial or personal relationship with other people or organizations that could inappropriately influence or bias the content of the paper.
- It is to specifically state that "No Competing interests are at stake and there is No Conflict of Interest" with other people or organizations that could inappropriately influence or bias the content of the paper.

References

[1] Y. Karzazi, Organic light emitting diodes: devices and applications, J. Mater. Environ. Sci. 5 (2014) 1–12.
[2] Y. Luo, S. Li, Y. Zhao, C. Li, Z. Pang, Y. Huang, M. Yang, L. Zhou, X. Zheng, X. Pu, Z. Lu, An ultraviolet thermally activated delayed fluorescence OLED with total external quantum efficiency over 9%, Adv. Mater. 32 (2020) 2001248–2001253, https://doi.org/10.1002/adma.202001248.
[3] R. Yankova, I. Tankov, NLO response as a function of structural water presence: a comparative experimental (UV–vis) and DFT (structural, NPA, MEP) study on Cs2Ni(SeO4)2•4H2O and Cs2Ni(SeO4)2, J. Mol. Struct. 1224 (2021) 129047–129058, https://doi.org/10.1016/j.molstruc.2020.129047.
[4] H. Derouiche, V. Djara, Impact of the energy difference in LUMO and HOMO of the bulk heterojunctions components on the efficiency of organic solar cells, Sol. Energy Mater. Sol. Cells 91 (2007) 1163–1167, https://doi.org/10.1016/j.solmat.2007.03.015.
[5] M. Bourass, A.T. Benjelloun, M. Benzakour, F. M.Mcharfi, F.S. Jhilal, M. Hamidi, M. Bouachrine, The optoelectronic properties of organic materials based on triphenylamine that are relevant to organic solar photovoltaic cells, New J. Chem. 22 (2017) 563–574, https://doi.org/10.1039/C7NJ03272B.
[6] M.C. Gather, S. Reineke, Recent advances in light outcoupling from white organic light-emitting diodes, J. Photonics Energy 5 (2015), https://doi.org/10.1117/1.jpe.5.057607 (57607-57607).
[7] R. Luo, H. Li, B. Du, S. Zhou, Y. Zhu, A simple strategy for high stretchable, flexible and conductive polymer films based on PEDOT: PSS-PDMS blends, Org. Electron. 76 (2020), 105451, https://doi.org/10.1016/j.orgel.2019.105451.
[8] J. Bauri, R.B. Choudhary, G. Mandal, Recent advances in efficient emissive materials-based OLED applications: a review, J. Mater. Sci. 56 (2021) 18837–18866, https://doi.org/10.1007/s10853-021-06503-y.
[9] Y. Wang, L. Ping, H. Wang, Z. Baoqing, W. Jianghao, C. Feng, Flexible organic lightemitting devices with copper nanowire composite transparent conductive electrode, J. Mater. Sci. 54 (2019) 2343–2350, https://doi.org/10.1007/s10853-018-2986-9.
[10] M. Zhang, L. Zhao, R. Zhao, Z. Li, Y. Liu, Y. Duan, Tianyu Han, A mechanochromic luminescent material with aggregation-induced emission: application for pressure sensing and mapping, Spectrochim. Acta Part A: Mol. Biomol. Spectrosc. 220 (2019), 117125, https://doi.org/10.1016/j.saa.2019.05.030.
[11] J.K.J. Van Duren, X. Yang, J. Loos, C.W.T. Bulle-Lieuwma, A.B. Sieval, J.C. Hummelen, R.A.J. Janssen, Relating the morphology of poly(p-phenylene vinylene)/methanofullerene blends to solar-cell performance, Adv. Funct. Mater. 14 (2004) 425–434, https://doi.org/10.1002/adfm.200305049.
[12] H. Hoppe, M. Niggemann, C. Winder, J. Kraut, R. Hiesgen, A. Hisch, D. Meissner, N.S. Sariciftci, Adv. Funct. Mater. 14 (2004) 1005–1011, https://doi.org/10.1002/adfm.200305049.
[13] B.C. Jeon, M.S. Kim, M.J. Cho, D.H. Choi, K.-S. Ahn, J.H. Kim, Effect of solvent on dye-adsorption process and photovoltaic properties of dendritic organic dye on TiO2 electrode of dye-sensitized solar cells, Synth. Met. 188 (2014) 130–135, https://doi.org/10.1016/j.synthmet.2013.12.006.
[14] Y. Liu, H.C. Du, G. Wang, X. Gong, L. Wang, H. Xiao, Theoretical investigation of solvent effects on tautomeric equilibrium of 2-diazo-4,6-dinitrophenol, Int. J. Quant. Chem. 111 (2011) 1115–1126, https://doi.org/10.1002/qua.22468.
[15] M.J. Frisch, G.W. Trucks, H.B. Schlegel, G.E. Scuseria, M.A. Robb, J.R. Cheeseman, G. Scalmani, V. Barone, B. Mennucci, G. Petersson, et al., Gaussian 09, Revision A.2, Gaussian, Inc., Wallingford CT, 2009.
[16] R. Dennington, T. Keith, J. Millam, GaussView, Version 5, Semichem Inc., Shawnee Mission KS, 2009.
[17] M. Jamal, N. Kamali Sarvestani, A. Yazdani, A.H. Reshak, Mechanical and thermodynamical properties of hexagonal compounds at optimized lattice parameters from two-dimensional search of the equation of state, RSC Adv. 4 (2014) 57903–57915, https://doi.org/10.1039/C4RA09358E.
[18] A.H. Reshak, D. Stys, S. Auluck, I.V. Kityk, Dispersion of linear and nonlinear optical susceptibilities and the hyperpolarizability of 3-methyl-4-phenyl-5-(2-pyridyl)-1,2,4-triazole, Phys. Chem. Chem. Phys. 13 (2011) 2945–2952, https://doi.org/10.1039/C0CP01601B.
[19] G.W. Ejuh, F. Tchangnwa Nya, M.T. Ottou Abe, F.F. Jean-Basptiste, J.M.B. Ndjaka, Electronic structure, physico-chemical, linear and non linear optical properties analysis of coronene, 6B-, 6N-, 3B3N- substituted C24H12 using RHF, B3LYP and wB97XD methods, Opt. Quant. Electron. 49 (2017) 382–389, https://doi.org/10.1007/s11082-017-1221-2 2017.
[20] C.E. Ndikilar, L.S. Taura, G.W. Ejuh, A. Muhammad, RHF and DFT study of the molecular and electronic properties of (SiO2)n and (GeO2)n nanoclusters, Mod. Appl. Sci. 12 (2018) 108–118, https://doi.org/10.5539/mas.v12n9p108.
[21] F. Tchangnwa Nya, G.W. Ejuh, J.M.B. Ndjaka, Theoretical study of optoelectronic and thermodynamic properties of molecule 4-[2-(2-N,N-dihydroxy amino thiophene)vinyl]benzanamine: Influence of hydroxyl position, Mater. Lett. 202 (2017) 89–95, https://doi.org/10.1016/j.matlet.2017.05.064.
[22] J.B.F. Fankam, G.W. Ejuh, F. Tchangnwa Nya, J.M.B. Ndjaka, Study of electronic structure, optoelectronics, linear and nonlinear optical properties and chemical descriptors of dibromodinitrofluorescein isomers in gasphase and solvent media using abinitio and DFT methods, Chin. J. Phys. 66 (2020) 461–473, https://doi.org/10.1016/j.cjph.2020.05.015.
[23] J.C. Fan, Z.C. Shang, J. Liang, X.H. Liu, H. Jin, Systematic theoretical investigations on the tautomers of thymine in gas phase and solution, J. Mol. Struct.–Theochem. 939 (2010) 106–111, https://doi.org/10.1016/j.theochem.2009.09.047.
[24] R.M. Abozaid, Z. Lazarević, I. Radović, M. Gilić, D. Šević, M.S. Rabasović, V. Radojević, Optical properties and fluorescence of quantum dots CdSe/ZnSPMMA composite films with interface modifications, Opt. Mater. 92 (2019) 405–410, https://doi.org/10.1016/j.optmat.2019.05.012.
[25] M.B. Mohamed, M.H. Abdel-Kader, Effect of annealed ZnS nanoparticles on the structural and optical properties of PVA polymer nanocomposite, Mater. Chem. Phys. 241 (2020), 122285, https://doi.org/10.1016/j.matchemphys.2019.122285.
[26] P.A. Ajibade, J.Z. Mbese, Synthesis and characterization of metal sulfides nanoparticles/poly(methyl methacrylate) nanocomposites, Int J. Polym. Sci. 2014 (2014) 1–8, 10. 1155/2014/752394.
[27] T. Hasegawa, J. Takeya, Organic field-effect transistors using single crystals, Sci. Technol. Adv. Mater. 10 (2009), https://doi.org/10.1088/1468-6996/10/2/024314.
[28] D.R. Lee, S.H. Hwang, S.K. Jeon, C.W. Lee, J.Y. Lee, Benzofurocarbazole and benzothienocarbazole as donors for improved quantum efficiency in blue thermally activated delayed fluorescent devices, Chem. Commun. 51 (2015) 8105–8107, https://doi.org/10.1039/C5CC01940K.
[29] J. Tauc, Amorphous and Liquid Semiconductors, Plenum Press, New York, 1974.
[30] P. S.Georges, H.S. Zhenhua, Chapter three – III–V semiconductor photoelectrodes, Semicond. Semimet. 97 (2017) 81–138, https://doi.org/10.1016/bs.semsem.2017.03.002.
[31] J. Schneider, M. Matsuoka, M. Takeuchi, J. Zhang, Y. Horiuchi, M. Anpo, D.W. Bahnemann, Understanding TiO2 photocatalysis mechanisms and materials, Chem. Rev. 114 (2014) 9919–9986, https://doi.org/10.1021/cr5001892.

[32] J. Jin, R. Qi, Y. Su, M. Tong, J. Zhu, Preparation of high-refractive index PMMA/TiO2 nanocomposites by one-step in situ solvothermal method, Iran. Polym. J. 22 (2013) 767–774, https://doi.org/10.1007/s13726-013-0175-x.
[33] Z. Yang, H. Peng, W. Wang, T. Liu, Crystallization behavior of poly(e-caprolactone)-layered double hydroxide nanocomposites, J. Appl. Polym. Sci. 116 (2010) 2658–2667, https://doi.org/10.1002/app.
[34] B.H. Rabee, B.A. Al-kareem, Study of optical properties of (PMMA-CuO) nanocomposites, Int. J. Sci. Res. 5 (2016) 879–883.
[35] E. Tanış, N. Çankaya, Electronic, optical and non-linear optical properties of an cyclohexylacrylamide molecule: a potential optoelectronic agent, Opto-Electron. Rev. 28 (2020) 74–81, https://doi.org/10.24425/opelre.2020.135257.
[36] A. Lamichhane, N.M. Ravindra, Energy gap-refractive index relations in perovskites, Materials 13 (2020) 1917, https://doi.org/10.3390/ma13081917.
[37] N. Ravindra, S. Auluck, V. Srivastava, On the penn gap in semiconductors, Phys. Status Solidi B 93 (1979) K155–K160, https://doi.org/10.1002/pssb.2220930257.
[38] P. Herve, L. Vandamme, General relation between refractive index and energy gap in semiconductors, Infrared Phys. Technol. 35 (1994) 609–615, https://doi.org/10.1016/1350-4495(94)90026-4.
[39] R. Reddy, S. Anjaneyulu, Analysis of the Moss and Ravindra relations, Phys. Status Solidi B 174 (1992) K91–K93, https://doi.org/10.1002/pssb.2221740238.
[40] E. Sharma, P. Sharma, Applicability of different models of energy bandgap and refractive index for chalcogenide thin films, Mater. Today: Proc. 28 (2020) 92–95, https://doi.org/10.1016/j.matpr.2020.01.342.
[41] G. Chartier, Optics Handbook, Hermes, Paris, 1997.
[42] O. Renault, O.V. Salata, M. Etchells, P.J. Dobson, V. Christou, A low reflectivity multilayer cathode for organic light-emitting diodes, Thin Solid Films 379 (2000) 195–198, https://doi.org/10.1016/S0040-6090(00)01558-3.
[43] Asim Mantarcı, Changes in optical and sensing properties of 26DCzPPy WOLED material for different molarities, Opt. Quantum Electron. 53 (2021), https://doi.org/10.1007/s11082-020-02673-2 (pp. 53-31).
[44] P.R. Bhattacharjee, Refinement of the definitions of angles of incidence, reflection, refraction, and critical angle in ray optics, Optik 172 (2018) 1187–1192, https://doi.org/10.1016/j.ijleo.2018.06.144.
[45] A. Purniawan, G. Pandraud, T.S.Y. Moh, A. Marthen, K.A. Vakalopoulos, P.J. French, P.M. Sarro, Fabrication and optical measurements of a TiO2-ALD evanescent waveguide sensor, Sens. Actuators A Phys. 188 (2012) 127–132, https://doi.org/10.1016/j.sna.2012.05.037.
[46] Asim Mantarcı, Solvent effects on optical properties of 26DCzPPy material, Optik 224 (2020), 165709, https://doi.org/10.1016/j.ijleo.2020.165709.